

One-loop Evolution of a Rolling Tachyon

Xingang Chen*

*Institute for Fundamental Theory
Department of Physics, University of Florida, Gainesville, FL 32611*

Abstract

We study the time evolution of the one-loop diagram in Sen's rolling tachyon background. We find that at least in the long cylinder case they grow rapidly at late time, due to the exponential growth of the timelike oscillator terms in the boundary state. This can also be interpreted as the virtual open string pair creation in the decaying brane. This behavior indicates a breakdown of this rolling tachyon solution at some point during the evolution. We also discuss the closed string emission from this one-loop diagram, and the evolution of a one-loop diagram connecting a decaying brane to a stable brane, which is responsible for the physical open string creation on the stable brane.

*email address: xgchen@phys.ufl.edu

I. INTRODUCTION

Brane decay [1] is an important process in string theory. But the dynamics of this process is difficult to study at a fundamental level because it is both non-perturbative and of high energy. Recently Sen [2,3] has proposed a boundary conformal field theory (BCFT) description of the rolling tachyon which opens up a way to study the string dynamics in brane decay more quantitatively.

Sen proposed that adding a timelike sine-Gordon type boundary operator at open string end corresponds to a tachyon rolling down from an inverted potential. The corresponding boundary state is exactly solvable and has a marginal parameter describing the starting place of the rolling tachyon. Using this boundary state, he showed that, in the absence of the closed string coupling, the unstable brane decays into a pressureless matter called tachyon matter [2–4].

To better understand the nature of this tachyon matter, closed string coupling is studied in [5–7]. By calculating the one-point function on a disk in the rolling tachyon background, it is found [7,8] that a coherent state of heavy closed strings is produced during the brane decay. For the D p -brane with $p \leq 2$, the leading order of the emitted energy is infinite. Therefore all the energy goes to the closed strings localized at the original place of the unstable brane.¹ This is the closed string description of the tachyon matter [9,10]. For $p > 2$, the emitted energy is finite and thus of lower order in string coupling comparing to the brane tension. It is argued [7,8] that physically since the long wavelength tachyon modes will grow and eventually make these branes become causally disconnected D0-branes [11,12], they will also all decay into closed strings. But how fast this can happen presumably depends on the initial homogeneity condition of the brane, and if we start with sufficiently homogeneous brane, the tachyon matter may still show up.

The mini-superspace approximation [13–15] has been used [16–19] to study the open string creation from the rolling tachyon. In this approximation the size of the open string is neglected and the tachyon vertex operator corresponds to an exponentially growing potential for the open string. It is found that the production of the open strings from this background grows exponentially for large time t . The closed string coupling is not considered in this approximation. However since the end product of the decaying brane no longer have the

¹More precisely, if we cut off the closed string energy at the order of $1/g$ so that it does not exceed the brane tension, for D0-brane, the emitted energy is of the same order of the brane. For $p > 0$ the emitted energy after this cutoff is of lower order in g .

open string degrees of freedom, the closed strings have to be produced from the open strings.

In this paper we consider the virtual open string pair production and its subsequent coupling to closed strings. This is the closed string production from a cylinder diagram with both ends on the decaying brane.² This diagram is the quantum correction, at the order of the string coupling g , of the one-point function on the disk.³

We first study the evolution of this cylinder diagram. We restrict ourself to the long cylinder case where the analytical results are simple. As we will see, this diagram grows rapidly for large t , due to the exponentially growing timelike oscillator modes [5] in Sen's boundary state. This is the indication that, if we consider the closed string emission from this quantum effect, the brane energy will all be converted to closed strings, regardless of the spatial dimension of the brane. This also indicates that the back reaction will have to modify the late time behavior of this boundary state, especially these timelike oscillator modes, i.e. these growing modes have to die down when all the energy is emitted.

By simply imposing a cutoff on the time evolution of the boundary state, we estimate the magnitude of the closed string production. We find it diverges very rapidly as the string level increases and may overwhelm the classical results. However the details are not clear yet, since we only have results for long cylinder case and the cutoff is too simple.

Open string creation will become physical if a stable brane is added. We will study the evolution of a one-loop diagram with one end on the rolling tachyon state and another on the Neumann boundary state. This diagram is responsible for the open string production on the stable brane from the decaying brane.

This paper is organized as follows. In Sec. II we review Sen's construction of the rolling tachyon boundary state. In Sec. III we illustrate our calculation for a long cylinder in a space-like case with both ends on a D-brane. We use this method to study the one-loop evolution in rolling tachyon in Sec. IV, we also discuss the closed string production and the one-loop evolution if one end is replaced by the Neumann boundary condition. Sec. V is the conclusion. In Appendix A, we calculate the one-point function on a cylinder exactly with various simple boundary conditions and compare them with the result in Sec. III. In Appendix B, we supply some calculations skipped in Sec. IV B. For simplicity we restrict our discussions to the bosonic string theory.

²Another possible way of getting closed strings from open strings is discussed in [20,21].

³Loop corrections and multiple-point functions for decaying brane in two dimensional string theory is recently studied in [22]. Another related discussion on the loop diagram is in [23].

II. REVIEW OF SEN'S DESCRIPTION

We first review Sen's BCFT description of the rolling tachyon. We start by introducing the exact solution [24,25] of a spacelike CFT with a sine-Gordon boundary interaction at $\sigma = 0$. The action of this BCFT is given by

$$S = \frac{1}{2\pi} \int dz d\bar{z} \partial X \bar{\partial} X - \tilde{\lambda} \int d\tau \cos X (\sigma = 0) . \quad (2.1)$$

The exact solution of the boundary state is found to be

$$|B\rangle = \sum_j \sum_{m=-j}^j \mathcal{D}_{m,-m}^j |j; m, m\rangle , \quad (2.2)$$

where $|j; m, m\rangle$ is the Ishibashi states [26] associated with the primary states $|j; m, m\rangle = |j, m\rangle_L |j, m\rangle_R$, and $\mathcal{D}_{m,-m}^j$ is the SU(2) rotation matrix element

$$\mathcal{D}_{m,-m}^j = \langle j, m | e^{i\pi\tilde{\lambda}(J_+ + J_-)} |j, -m\rangle . \quad (2.3)$$

It is useful to express the states $|j, m\rangle_L \sim (J_-)^{j-m} |j, j\rangle_L$ explicitly in terms of the oscillators and zero modes using the chiral SU(2) generators [27–29]

$$J_{\pm} = \oint \frac{dz}{2\pi i} e^{\pm 2iX(z)} , \quad J_3 = \oint \frac{dz}{2\pi i} i\partial X(z) , \quad (2.4)$$

and

$$|j, j\rangle_L = e^{2ijX(0)} |0\rangle . \quad (2.5)$$

Similar expressions hold for the anti-holomorphic states $|j, m\rangle_R$.

The physically inequivalent solution is described by $-\frac{1}{2} \leq \tilde{\lambda} < \frac{1}{2}$. The $\tilde{\lambda} = 0$ case corresponds to the Neumann boundary condition. For $\tilde{\lambda} = -\frac{1}{2}$, this boundary state describes a periodic array of D-branes located at $x = 2n\pi$. For $\tilde{\lambda} = \frac{1}{2}$, this D-brane array is shifted to $x = (2n+1)\pi$. General $\tilde{\lambda}$ interpolates between the Neumann and Dirichlet boundary conditions.

Each primary state can be expanded into a zero mode e^{2imx} times oscillators of level $j^2 - m^2$ using (2.4) and (2.5). For example, the oscillator-free term in (2.2) is contributed by the primary states $|j; \pm j, \pm j\rangle$. It is given by

$$\tilde{f}(x) = 1 + \sum_{j=\frac{1}{2}, 1, \dots} (-\sin \tilde{\lambda}\pi)^{2j} (e^{2ijx} + e^{-2ijx}) \quad (2.6)$$

$$= \frac{1}{1 + e^{ix} \sin(\tilde{\lambda}\pi)} + \frac{1}{1 + e^{-ix} \sin(\tilde{\lambda}\pi)} - 1 , \quad (2.7)$$

where we denote x as the zero mode of X .

After the inverse Wick rotation $X \rightarrow -iX^0$, the boundary interaction term in (2.1) becomes a tachyon vertex operator

$$T(X^0) = \tilde{\lambda} \cosh X^0 . \quad (2.8)$$

In the vicinity of $t = 0$, this corresponds to a tachyon field $T(t)$ with

$$T(t = 0) = \tilde{\lambda} , \quad \dot{T}(t = 0) = 0 , \quad (2.9)$$

where t is the zero mode of X^0 . Since this time-like BCFT is also exactly solvable by inverse Wick rotating (2.2), the corresponding boundary state together with the spatial and ghost parts

$$|B\rangle = \mathcal{N}_p |B\rangle_{X^0} \otimes |B\rangle_{\vec{X}} \otimes |B\rangle_{bc} \quad (2.10)$$

should describe the long time evolution of the rolling tachyon.⁴

We notice that, after the inverse Wick rotation, the series (2.6) is only convergent for $t < |\log \sin \tilde{\lambda}\pi|$. However since this series can be summed into a closed form (2.7), the inverse Wick rotation is well defined for all t in (2.7). This term together with the next higher level term

$$|B\rangle_{X^0} = f(t)|0\rangle + g(t)\alpha_{-1}^0\tilde{\alpha}_{-1}^0|0\rangle + \dots , \quad (2.11)$$

where

$$f(t) = \frac{1}{1 + e^t \sin(\tilde{\lambda}\pi)} + \frac{1}{1 + e^{-t} \sin(\tilde{\lambda}\pi)} - 1 , \quad (2.12)$$

$$g(t) = \cos(2\tilde{\lambda}\pi) + 1 - f(t) , \quad (2.13)$$

are especially interesting because they are related to the stress tensor of the decaying brane by

$$T_{00} = \frac{1}{2}T_p(f(t) + g(t)) , \quad T_{ij} = -T_p f(t) \delta_{ij} , \quad (2.14)$$

where T_p is the brane tension and i, j denotes the longitudinal direction of the brane. Therefore, in the absence of the string coupling g , this boundary state describes a system with

⁴In this paper, we consider the full-brane, which is time reflection symmetric about $t = 0$. The $t < 0$ part describes the formation of a unstable brane, and the $t > 0$ part describes the decay of the brane. The boundary state of the half-brane case is given in [16,12,17].

conserved energy and becoming pressureless as $t \rightarrow \infty$. The special case $\tilde{\lambda} = \frac{1}{2}$ corresponds to delta functions on the imaginary axis and has no support on real t -axis. Correspondingly both $f(t)$ and $g(t)$ vanish.

If we consider higher oscillator level terms in (2.11), for a given level l , there are only finite number of primary states satisfying $j^2 - m^2 < l$ ($m \neq \pm j$). Therefore the sum of them is still exponentially dependent of t [5], unlike the $f(t)$ in (2.12) whose t -dependence is much milder.

Since the timelike oscillator part of a on-shell closed string state should be gauged away [7,30,31], the above mentioned exponentially growing modes do not show up in the one-point function of the disk amplitude for physical string emission. However it can contribute when an off-shell closed string is produced and affect the on-shell closed string production from a one-loop diagram. This will be the focus of this paper. One of the difficulties is that this diagram will sum over a series of exponential terms involving powers of e^t . If this summation diverges for a given t , one cannot conclude anything since a redefinition of the summation may be needed to bring it to a closed form like we did for (2.12). The main observation in this paper is that at least for the long cylinder case we find the summation to be convergent, and that the time-dependent behavior for this case is very different from that in the disk case.

III. SPACELIKE ONE-LOOP

As we have seen in Sec. II, the boundary state (2.2) defined by the BCFT (2.1) has a spatial dependence. For the oscillator-free component, the Fourier modes of such a dependence are given by the one-point function $\langle e^{ikX} \rangle$ on the disk. In this section to illustrate our method we will study the amplitude $\langle e^{ikX} \rangle$ on an Euclidean cylinder.

Since the boundary state is known, this open string one-loop diagram can be calculated in terms of closed strings. A state corresponding to the vertex operator e^{ikX} is emitted during the closed string propagation from one boundary state to another. The amplitude is then

$$\begin{aligned} \tilde{A}_{BB}(k) &= \langle B | q_1^{L_0 + \tilde{L}_0} e^{ikX} q_2^{L_0 + \tilde{L}_0} | B \rangle \\ &\equiv \int dx e^{ikx} A_{BB}(x) , \end{aligned} \quad (3.1)$$

where $q_{1,2} = e^{-2\pi s_{1,2}}$ and the x is the zero-mode of the X . In the second line we have denoted the Fourier transform of this amplitude as $A_{BB}(x)$. $A_{BB}(x)$ is also dependent of the moduli $s_{1,2}$.

For a boundary state (2.2) with general $\tilde{\lambda}$, this is still difficult to calculate since the vertex operator e^{ikX} includes all the oscillator modes which must be contracted with those from the boundary states. But the calculation is simplified as $s_{1,2}$ become large. Comparing to the zero mode contribution in e^{ikX} , the oscillator contributions are of higher order in $q_{1,2}$, thus get suppressed if $s_{1,2} \gg 1$. That is, we will study the following amplitude

$$\langle B | q_1^{L_0 + \tilde{L}_0} e^{ikx} q_2^{L_0 + \tilde{L}_0} | B \rangle . \quad (3.2)$$

To give an example we study the case of a single D0-brane located at $x = 0$

$$|D\rangle = \delta(x) e^{\sum_{n=0}^{\infty} \frac{1}{n} \alpha_{-n} \tilde{\alpha}_{-n}} |0\rangle . \quad (3.3)$$

Using the approximation (3.2) we get

$$\begin{aligned} \tilde{A}_{DD}(k) &\approx \langle D | q_1^{L_0 + \tilde{L}_0} e^{ikx} q_2^{L_0 + \tilde{L}_0} | D \rangle \\ &\approx \frac{1}{4\pi^2} \int dp \, q_1^{(p-k)^2/2} q_2^{p^2/2} \end{aligned} \quad (3.4)$$

$$= \frac{1}{4\pi^2} \frac{1}{\sqrt{s}} e^{-\pi k^2 s_1 s_2 / s} . \quad (s = s_1 + s_2) \quad (3.5)$$

Fourier transforming it to the coordinate space, we get

$$\begin{aligned} A_{DD}(x) &\approx \frac{1}{8\pi^3} \int dp_1 dp_2 \, q_1^{p_1^2/2} q_2^{p_2^2/2} e^{i(p_1 - p_2)x} \\ &= \frac{1}{8\pi^3} \frac{1}{\sqrt{s_1 s_2}} e^{-\frac{x^2}{4\pi} \left(\frac{1}{s_1} + \frac{1}{s_2} \right)} . \end{aligned} \quad (3.6)$$

Different from the disk amplitude, the one-loop amplitude is no longer localized at $x = 0$. Physically this is due to the closed string propagating off the D-brane and then coming back. This propagation is parameterized by the moduli $s_{1,2}$. From (3.6) we can see that as $s_{1,2}$ decrease the amplitude gets more localized toward the location of the brane.

In Appendix A we will verify (3.5) using the exact result.

IV. ONE-LOOP EVOLUTION

A. One-loop for rolling tachyon

To study the closed string production from the cylinder diagram, we will be interested in the quantity $\langle e^{iEX^0} \rangle_{\text{cylinder}}$. The boundaries of this cylinder are given by Sen's rolling tachyon boundary state $|B\rangle_{X^0}$. This quantity gives the timelike component of the physical closed string emission. Similar to Sec. III, we will denote the Fourier transform of $\langle e^{iEX^0} \rangle_{\text{cylinder}}$ as

$A_{BB}(t)$ and think of it as a time evolution of the one-loop diagram with moduli $s_{1,2}$. Again, we will concentrate on the long cylinder case where we only take the zero mode of this vertex operator,⁵ namely e^{iEt} . We will be interested in the small $\tilde{\lambda}$ case and this corresponds to placing the tachyon near the top of the potential.

Using the explicit form of the boundary state $|B\rangle_{X^0}$ given by inverse Wick rotating (2.2), we have

$$\tilde{A}_{BB}(E) \equiv \int dt e^{iEt} A_{BB}(t) \quad (4.1)$$

$$\approx_{X^0} \langle B | q_1^{L_0+\tilde{L}_0} e^{iEt} q_2^{L_0+\tilde{L}_0} | B \rangle_{X^0} \quad (4.2)$$

$$= \sum \mathcal{D}_{m_1, -m_1}^{j_1} \mathcal{D}_{m_2, -m_2}^{j_2} \langle j_1; m_1, m_1 | q_1^{L_0+\tilde{L}_0} e^{iEt} q_2^{L_0+\tilde{L}_0} | j_2; m_2, m_2 \rangle \rangle_{X^0} . \quad (4.3)$$

Note an integration over t is implicit in the last two lines. Since only the zero mode e^{iEt} enters in (4.3), $A_{BB}(t)$ can be read off from (4.3) before doing the integration $\int dt e^{iEt} \dots$. However as we will see, although $A_{BB}(t)$ turns out to be convergent for a given t , it blows up as $t \rightarrow \infty$. Therefore a upper limit of the integration over t has to be specified on physical grounds.

To perform the summation in (4.3), we have to distinguish two different cases. The first case is when $m_1 = \pm j_1$ and $m_2 = \pm j_2$. We denote this subspace of $|B\rangle_{X^0}$ as $|B^0\rangle$. As we see from Sec. II, for the primary states, this is an infinite series of oscillator-free terms. It only makes sense if we sum them over to a closed form before we do the inverse Wick rotation. Therefore in (4.3) we should use the form (2.12) rather than treat these terms individually. The descendent states can be built by acting the Virasoro generators on this primary state

$$\sum_{\{n_m\}} \prod_{m>0} \left(L_{-m} \tilde{L}_{-m} \right)^{n_m} f(t) |0; 0, 0\rangle . \quad (4.4)$$

In our long cylinder case, to get the leading term we only need to look at the primary states, because the descendent states give rise to terms higher order in $q_{1,2}$. Hence We get

$$\langle B^0 | q_1^{L_0+\tilde{L}_0} e^{iEt} q_2^{L_0+\tilde{L}_0} | B^0 \rangle \approx \int dt e^{iEt} \left(q_1^{\frac{1}{2} \frac{\partial^2}{\partial t^2}} f(t) \right) \left(q_2^{\frac{1}{2} \frac{\partial^2}{\partial t^2}} f(t) \right) . \quad (4.5)$$

So this case contributes to $A_{BB}(t)$ a term

$$A_{BB}^{B^0}(t) \approx \left(q_1^{\frac{1}{2} \frac{\partial^2}{\partial t^2}} f(t) \right) \left(q_2^{\frac{1}{2} \frac{\partial^2}{\partial t^2}} f(t) \right) . \quad (4.6)$$

⁵An exception is discussed in footnote 8.

The second case includes the rest of the terms in $|B\rangle_{X^0}$. We denote it as $|\tilde{B}\rangle$. The contraction of these terms give⁶

$$\begin{aligned} & \langle \tilde{B} | q_1^{L_0 + \tilde{L}_0} e^{iEt} q_2^{L_0 + \tilde{L}_0} | \tilde{B} \rangle \\ & \approx \sum_{m_{1,2} \neq \pm j_{1,2}} \mathcal{D}_{m_1, -m_1}^{j_1} \mathcal{D}_{m_2, -m_2}^{j_2} \langle j_1; m_1, m_1 | e^{iEt} | j_2; m_2, m_2 \rangle q_1^{2j_1^2} q_2^{2j_2^2}. \end{aligned} \quad (4.7)$$

The factor $q_1^{2j_1^2} q_2^{2j_2^2}$ is obtained by acting $q_{1,2}^{L_0 + \tilde{L}_0}$ on the primary states.⁷ For small $\tilde{\lambda}$,

$$\mathcal{D}_{m, -m}^j \approx \frac{(j + |m|)!}{(j - |m|)! (2|m|)!} (i \sin \tilde{\lambda} \pi)^{2|m|}. \quad (4.8)$$

The primary states $|j; m, m\rangle$ consist of the zero modes e^{2mt} and the oscillator modes of level $j^2 - m^2$. So in (4.7) the quantity

$$\begin{aligned} & \langle j_1; m_1, m_1 | e^{iEt} | j_2; m_2, m_2 \rangle \\ & = n(j_1, j_2, m_1, m_2) \delta_{j_1^2 - m_1^2, j_2^2 - m_2^2} \int dt e^{iEt} e^{2(m_2 + m_1)t}, \end{aligned} \quad (4.9)$$

where the oscillator levels have to match to give a non-zero answer⁸ and we use $n(j_1, j_2, m_1, m_2)$ to denote the number resulted from the contraction between two normalized oscillator states of the same level. Besides some special values of j and m , the delta function in (4.9) is non-zero for $j_1 = j_2 = j$ and $m_1 = \pm m_2$ ($m_1 \neq \pm j_1$ and $m_2 \neq \pm j_2$).

Combining (4.7) and (4.9) we can read off

$$A_{BB}^{\tilde{B}}(t) \approx \sum_{j, m_1 = \pm m_2} \tilde{n} q^{2j^2} e^{-2\tau_\lambda(|m_1| + |m_2|)} e^{2(m_2 + m_1)t}, \quad (q = q_1 q_2) \quad (4.10)$$

⁶There are no cross terms between $|B^0\rangle$ and $|\tilde{B}\rangle$ in (4.2) since the corresponding primary states have different oscillator levels.

⁷Note that here we have kept the different powers of $q_{1,2}$, each of which is the leading term, contributing by the primary states, over those from the descendent states for small $q_{1,2}$. However among these terms in (4.7), it is no longer true that the lowest $j_{1,2}$ gives the leading behavior. This is because, as we will see shortly, the quantity $\langle j_1; m_1, m_1 | e^{iEt} | j_2; m_2, m_2 \rangle$ exponentially grows as $j_{1,2}$ grows. Also because of this, in (4.7) and the subsequent (4.10), we will be interested only in the leading term.

⁸Here the vanishing contribution of the $j_1^2 - m_1^2 \neq j_2^2 - m_2^2$ case (including the cross term between $|B^0\rangle$ and $|\tilde{B}\rangle$) leaves the possibility of the contribution from the oscillator terms in e^{iEX^0} or the descendent states (they are needed to match the oscillator level for $j_1^2 - m_1^2 \neq j_2^2 - m_2^2$). Following the same spirit, one can see that their leading contribution comes from terms with minimal oscillators for fixed $e^{2m_{1,2}t}$, namely $j_1 = m_1 + 1, j_2 = m_2 + 1$ ($j_1 \neq j_2, m_{1,2} > 0$). After summation, its behavior ($\sim e^{(t - \tau_\lambda)^2(1/s_1 + 1/s_2)/4\pi}$) is similar to (4.12).

where we have defined

$$\tau_\lambda \equiv |\log(\sin \tilde{\lambda}\pi)| \quad (4.11)$$

and absorbed all the numerical and phases in \tilde{n} . Different from the series in (2.6) (with x replaced by $-it$), which is divergent and thus needs to be redefined for $t > \tau_\lambda$, we notice that in (4.10) the summation over j and m is convergent due to the factors of q^{2j^2} .

Since the full-brane is time reflection symmetric, we will only focus on the decay side $t > 0$. For $t \ll \tau_\lambda$, (4.6) is bigger than (4.10) and we have $A_{BB}(t) \approx 1$ because $f(t)$ has very weak t -dependence in this region. This contribution starts to decrease around $t \sim \tau_\lambda$ and is gradually taken over by (4.10). The leading term for $t - \tau_\lambda \gg 2\pi s$ is especially simple. This comes from the term with $m_2 = m_1 = j - 1 \approx \frac{t - \tau_\lambda}{2\pi s}$ in (4.10). Up to numerical factors and phases we have⁹

$$A_{BB}(t) \sim e^{(t - \tau_\lambda)^2/\pi s} \quad (t - \tau_\lambda \gg 2\pi s) . \quad (4.12)$$

Therefore $A_{BB}(t)$ in (4.1) is well defined for each t , but it grows rapidly as $t \rightarrow \infty$. This is the quantum property of the tachyon matter if the decaying brane does not completely go to the closed strings in the classical level. Different contour of the t -integration in (4.1) may correspond to different choice of vacua [7]. Since all the contour will go through the large value of the real t , we expect this qualitative behavior to be independent of the vacuum choice. Physically closed strings will be created from such a one-loop diagram and this rapid growth has to stop in a time scale τ during which all the brane energy is emitted.

Note that we have only considered the case where $s_{1,2}$ are large. In principle we should integrate over the moduli $s_{1,2}$. We see from (4.12) that when s decreases, $A_{BB}(t)$ increases, so it will only make the amplitude bigger. But the effect we are unable to take into account in this paper is that when $s_{1,2} \rightarrow 0$ the oscillator modes in e^{iEX^0} are no longer negligible. It is not clear, although unlikely, if the contribution of these modes can exactly cancel the leading order in (4.12). Another complication is when $s \rightarrow 0$, we will encounter the infrared divergence as suggested by (4.12). However if a time scale τ has to be imposed to this rolling tachyon evolution so that it is a finite time process, we should have a natural infrared cutoff on s , which is $s > 1/\tau$ (as well as infrared cutoff on closed string propagation, so $s < \tau$).

⁹This is reminiscent of the Euclidean cylinder, where we have a factor of $e^{-y^2/4\pi s}$ if the string is stretched by a distance y . The t -dependence here is like stretching a string in the time direction.

B. Closed string emission

The time-dependent boundary state provides a source for closed strings. At the classical level, this is described by the one-point function on the disk with the vertex operator representing the physical closed string state. The total energy emitted is proportional to the sum of the square of the amplitudes associated with all the physical states [32,7]. Because the contribution from the spacelike components are all equal to one for the disk case [7], the amplitude-square for different closed string states are the same. They scale as $e^{-2\pi E}$ for large E . This exponential damping factor is exactly cancelled by the exponential growing term in the Hagedorn density $\sim e^{2\pi E}$ and results in a power-law dependence of the total emitted energy on the string level n .

Here we regard the one-point function on the cylinder as the quantum correction to the above classical result. To proceed, we use the simplest cutoff τ on the evolution of the rolling tachyon. Therefore in (4.5) and (4.9) we integrate from $t = 0$ to $t = \tau$. The leading term for (4.1) scales as $1/E$ for high level states, which damps much slower than the disk case.¹⁰ Imposing smoother cutoff may reduce this amplitude. But as we will roughly see in Appendix B that, the spatial parts of the amplitudes for different emitted closed string states is no longer the same as they are in the disk case, they grow rapidly as the string level increases. Combining with the growth of the Hagedorn density, this will result in a rapid divergence in the emitted total energy as the closed string level increases. This may overwhelm the classical result and reduce the mass level of the emitted closed strings if the string coupling g is not sufficiently small.

Clearly, to study more details, we need to have a better understanding of the back reaction and more complete calculation of the loop diagram. Other channels, such as the two-point function on the disk and higher order diagrams also deserve further study.

C. Adding a spectator brane

In this subsection we consider the time evolution of a cylinder diagram with one boundary given by Sen's rolling tachyon state and another satisfying the Neumann boundary condition. As in the previous discussion we will concentrate on the timelike part, the spacelike part of the cylinder diagram is as usual [33]. Applied to the superstring theory, this corresponds to a one-loop diagram connecting a decaying brane and a stable brane. On the stable brane, open

¹⁰For $\tau - \tau_\lambda \gg 2\pi s$, there is also a factor of $e^{(\tau - \tau_\lambda)^2/\pi s}$ coming from the leading term in (4.9).

strings will be created if string coupling is considered. Since stable D-brane does not exist in the bosonic string theory that we will study, one can image that one brane is decaying much slower than another.

We have the choices of putting the vertex operator in the middle of the cylinder or on the Neumann boundary. We will calculate the latter as an example. We again restrict to the long cylinder case.

The amplitude is

$$\begin{aligned}\tilde{A}_{BN}(E) &\equiv \int dt e^{iEt} A_{BN}(t) \\ &\approx \langle B | q^{L_0 + \tilde{L}_0} e^{iEt} | N \rangle .\end{aligned}\quad (4.13)$$

The Neumann boundary state is given by [24]

$$|N\rangle = \sum_j |j; 0, 0\rangle \rangle . \quad (4.14)$$

As in Sec. IV, the constraint

$$j_1^2 - m_1^2 = j_2^2 \quad (4.15)$$

($m_2 = 0$ in this case) is satisfied by the following several cases. For $m_1 = \pm j_1$ and $j_2 = 0$, similar argument as in Sec. IV leads to a contribution to $A_{BN}(t)$ as

$$q^{\frac{1}{2} \frac{\partial^2}{\partial t^2}} f(t) . \quad (4.16)$$

This gives a relatively flat time evolution for $t < \tau_\lambda$, which means that the tachyon has not started to roll quickly and the boundary state is still close to Neumann boundary. The $j_1 = j_2 = j$ and $m_1 = m_2 = 0$ case gives a time-independent term $\approx q^{\frac{1}{2}}$ in $A_{BN}(t)$, which is quite different from (4.12). Therefore the special case which we did not consider in Sec. IV A becomes important here. These contribution will become dominant for large t . It is not difficult to see that the evolution for large t is much slower than (4.12). For example there are special values satisfying (4.15) with $m_1 \neq 0$ and $j_2 \neq 0$. Even if we assume that j_1 and m_1 is continuous, we will get $e^{(t-\tau_\lambda)^2/4\pi s}$ (at $j_1 \approx m_1 \approx (t - \tau_\lambda)/4\pi s$) which is much slower than (4.12) due to the time-independence of the Neumann boundary state. The situation is similar for cases with $j_1^2 - m_1^2 \neq j_2^2$. In addition if these two branes are separated by a distance y in the transverse direction, there will be another suppression factor $e^{-y^2/4\pi s}$ coming from the spacelike part of the diagram.

Including the spatial and ghost parts of the open string vertex operator, this one-point function on the Neumann boundary corresponds to the physical open string emission on the

spectator brane. We expect that a coherent state of massive open strings will be created. At the same time, the closed strings will also be created by inserting the closed string vertex operator in the bulk of this cylinder. It will be interesting to study these in more details and see how the energy of the decaying brane is distributed between the open and closed strings. This will have applications in various brane inflation models (see [34] for a review).

V. CONCLUSION

In this paper we have studied the one-loop evolution in the rolling tachyon background and the closed string emission from such a diagram. We calculated the long cylinder case where we approximate the vertex operator by its zero mode. In this case we show that the one-loop diagram will grow rapidly in time. This indicates that, if the tachyon matter survives the classical closed string emission, it will be converted to closed strings at quantum levels. The short cylinder, back reaction and other string emission channels have to be understood better to study more details of such a process.

It should be straightforward to extend the analyses in this paper to the half-brane case [16,12,17] and the superstring case [3,12]. It will also be interesting to study this when other backgrounds are present, such as the electric field [35–39] or spacelike linear dilation [40].

ACKNOWLEDGMENTS

I would like to thank Brandon Bates, Pei-Ming Ho, Zongan Qiu, Gary Shiu and Erick Weinberg for useful conversations. I am especially grateful to Dan Kabat, Ashoke Sen and Charles Thorn for many helpful discussions. This work was supported in part by the Department of Energy under Grant No. DE-FG02-97ER-41029.

APPENDIX A: ONE-POINT FUNCTIONS ON AN EUCLIDEAN CYLINDER

In this appendix, we compute the one-point functions on an Euclidean cylinder with the Dirichlet or Neumann boundary condition and compare these with the approximation we use in the paper.

1. DD boundary conditions

We start with the case of a single D-brane with a closed string tachyon vertex operator e^{ikX} . The length of the cylinder is $2\pi s$ and the circumference is 2π . This corresponds to

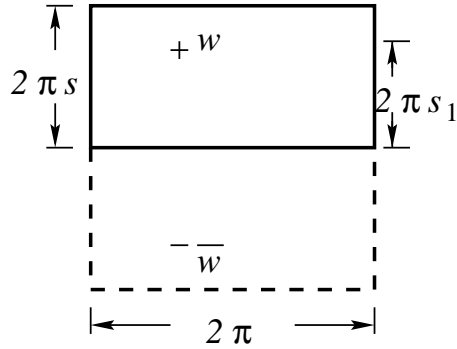


FIG. 1. The solid lines represents a cylinder of length $2\pi s$ and the circumference 2π . The left and right vertical boundaries are to be identified. Here both horizontal boundaries satisfy the Dirichlet boundary condition. The vertex operator is inserted at w . The extended diagram including the dash lines and the image of the vertex operator is the equivalent torus. The “+” and “-” signs represent the charges of the sources.

a strip in Fig. 1 with vertical boundaries identified. The vertex operator is at $w = 2i\pi s_1$. Because of the Dirichlet boundary condition, this source have images of opposite charges reflected by both horizontal boundaries. This is equivalent to a torus with periodicities 2π and $4\pi s$ and two opposite charges inserted at w and \bar{w} respectively. The self-contraction Green’s function is thus given by [41]

$$\begin{aligned} G'_r(w, w) &= \ln \left| 2\pi \frac{\theta_1(\frac{w-\bar{w}}{2\pi}, 2is)}{\theta'_1(0, 2is)} \right| - \frac{[\text{Im}(w - \bar{w})]^2}{8\pi s} \\ &= \ln \left| 2\pi \frac{\theta_1(2is_1, 2is)}{\theta'_1(0, 2is)} \right| - 2\pi \frac{s_1^2}{s}. \end{aligned} \quad (\text{A1})$$

The one-point function is then

$$\langle e^{ikX} \rangle = C_{DD} e^{-\frac{1}{2}k^2 G'_r(w, w)}, \quad (\text{A2})$$

where C_{DD} is the vacuum amplitude of the cylinder (neglecting an overall factor of $q^{-1/12}$)

$$C_{DD} = \frac{1}{4\pi^2 \sqrt{sh(q^2)}}, \quad (\text{A3})$$

where

$$h(q^2) = \prod_{n=1}^{\infty} (1 - q^{2n}). \quad (\text{A4})$$

We now look at this amplitude in different limits. It is useful to recall the formula [42]

$$\frac{\theta_1(\nu, \tau)}{\theta'_1(0, \tau)} = \frac{i}{2\pi} \frac{1-z}{\sqrt{z}} \prod_{n=1}^{\infty} \frac{(1 - q^n z)(1 - q^n z^{-1})}{(1 - q^n)^2}, \quad (\text{A5})$$

with

$$q = e^{2i\pi\tau}, \quad z = e^{2i\pi\nu}, \quad (\text{A6})$$

and it modular transformation

$$\frac{\theta_1(\nu, \tau)}{\theta_1'(0, \tau)} = -\tau e^{-i\pi\nu^2/\tau} \frac{\theta_1(-\nu/\tau, -1/\tau)}{\theta_1'(0, -1/\tau)}. \quad (\text{A7})$$

For $s_1, s_2 \gg 1$, using Eq. (A5), the one-point function (A2) goes to

$$\langle e^{ikX} \rangle \rightarrow C_{DD} e^{-\pi k^2 s_1 s_2 / s}. \quad (\text{A8})$$

In this limit, we recover the amplitude (3.5) as we expected.

We next consider the cases where s or s_1 gets small. In the first case we consider $s_1 \ll 1$ and $s_1/s \ll 1$ for given s . This corresponds to bring the vertex operator close to the boundary. In this case,

$$\langle e^{ikX} \rangle \rightarrow C_{DD} (4\pi s_1)^{-k^2/2}. \quad (\text{A9})$$

If we evaluate (A8) at this limit, we will get C_{DD} . So the actual result (A9) differs from it by a factor of $(4\pi s_1)^{-k^2/2}$, which diverges as $s_1 \rightarrow 0$.

The other case is that $s \ll 1$ but with s_1 comparable to s , i.e. $s_1/s \sim \text{const}$. In this case the cylinder becomes a long strip. This limit can be most easily studied using the modular transformation (A7) before using (A5). This gives

$$\langle e^{ikX} \rangle \rightarrow C_{DD} \left(4s \sin \pi \frac{s_1}{s} \right)^{-k^2/2}. \quad (\text{A10})$$

This differs from (A8) by a factor of $(4s \sin(\pi s_1/s))^{-k^2/2} \sim s^{-k^2/2}$. The infrared behavior in these two cases are similar.

2. DN boundary conditions

We consider the cylinder with one Dirichlet boundary and one Neumann boundary. We first consider the closed string insertion. This is equivalent to have four sources at $w, \bar{w}, \bar{w} + 4i\pi s$ and $w - 4i\pi s$ in a torus with periodicities 2π and $8\pi s$ (Fig. 2). The mirror images reflected by the Dirichlet boundary have the opposite charges, and those reflected by the Neumann boundary have the identical charges.

The one-point function is given by

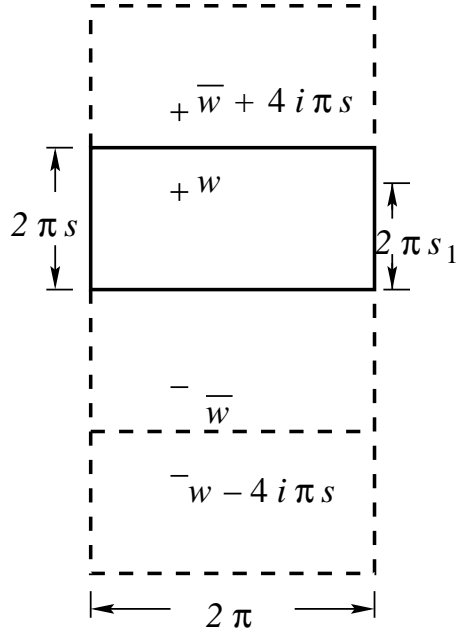


FIG. 2. Here the upper horizontal solid line represents Neumann boundary, and the lower one represents Dirichlet boundary. They give different image charges.

$$\langle e^{ikX} \rangle_{DN,c} = C_{DN} \left| 2\pi \frac{\theta_1(2is_1, 4is)}{\theta'_1(0, 4is)} \frac{\theta_1(2is, 4is)}{\theta_1(-2is_2, 4is)} \right|^{-k^2/2} e^{\pi k^2 s_1}, \quad (\text{A11})$$

where C_{DN} is the vacuum amplitude of the cylinder with DN boundary condition,

$$C_{DN} = \frac{1}{2\pi} \prod_{n=1}^{\infty} \frac{1}{(1 + q^{2n})}. \quad (\text{A12})$$

Taking the limit $s_1, s_2 \gg 1$, (A11) reduces to

$$C_{DN} e^{-\pi s_1 k^2} \quad (\text{A13})$$

This is the same as what we will get using the method in the paper

$$\langle D | q_1^{L_0 + \tilde{L}_0} e^{ikx} q_2^{L_0 + \tilde{L}_0} | N \rangle. \quad (\text{A14})$$

If the vertex operator gets close to the Dirichlet boundary ($s_1 \rightarrow 0, s_1/s \rightarrow 0$), or the cylinder becomes a long strip ($s \rightarrow 0, s_1/s \sim \text{const}$), we have the similar infrared behavior as in the last subsection with factors of $s_1^{-k^2/2}$ or $s^{-k^2/2}$. But if the vertex gets close to the Neumann boundary ($s_2 \rightarrow 0, s_2/s \rightarrow 0$), we will get a factor which vanishes as $s_2^{k^2/2}$.

Last we consider the cylinder with a vertex operator at the Neumann boundary. This is equivalent to a torus with opposite sources at $2i\pi s$ and $-2i\pi s$. Since these sources are at

the boundaries, the intensity is doubled because of the overlapped image sources. Similar calculation gives the one-point function

$$\langle e^{ikX} \rangle_{DN,o} = C_{DN} \left| 2\pi \frac{\theta_1(2is, 4is)}{\theta_1'(0, 4is)} \right|^{k^2} e^{\pi k^2 s}. \quad (\text{A15})$$

For large s , this gives

$$C_{DN} e^{-\pi k^2 s}, \quad (\text{A16})$$

which is the same as

$$\langle D | q^{L_0 + \tilde{L}_0} e^{ikx} | N \rangle. \quad (\text{A17})$$

As $s \rightarrow 0$, (A15) goes to

$$C_{DN} (8s)^{-k^2}. \quad (\text{A18})$$

This is the similar infrared behavior we encountered previously.

APPENDIX B: CLOSED STRING EMISSION FROM ONE-LOOP

As mentioned in Sec. IV B, in order to get the total emitted energy, we need to calculate the sum of the square of the amplitudes of all possible close string one-point functions. In this appendix we consider the contribution of the one-loop diagram. We shall give a rough estimate of the lower bound of this quantity and see its divergence.

For physical closed string states, the oscillator modes of the time-like component can be gauged away [7,30,31]. The one-point function then factorizes as

$$A = \langle e^{iEX^0} \rangle_{X^0} \langle V_{sp} \rangle_{\vec{x}}. \quad (\text{B1})$$

The first factor is the timelike component that we have studied in Sec. IV. The second factor is the spacelike component with the closed string vertex operator V_{sp} . The ghost part gives a time and state-independent factor, which is not included here. The evaluation of this part is more complicated than the disk case. For example, the amplitude for different closed string state is generally different, and the left and right oscillators do not have to be identical. For simplicity, we will study a subset of all possible closed string emission.

We consider the closed strings with oscillator modes only in one spatial direction, for example considering the Dirichlet boundary condition, and with zero transverse momenta and left-right identical oscillators

$$V_{sp} = \prod_m \left(-\frac{2m}{m!^2} \partial^m X \bar{\partial}^m X \right)^{n_m} . \quad (B2)$$

For these strings, the zero-modes contribution to the one-loop amplitude

$$\langle D | q_1^{L_0 + \tilde{L}_0} V_{sp} q_2^{L_0 + \tilde{L}_0} | D \rangle \quad (B3)$$

is proportional to

$$\int_{-\infty}^{\infty} dp \, q^{p^2/2} = \frac{1}{\sqrt{s}} . \quad (B4)$$

Let us only look at the lowest oscillator-modes in the corresponding vertex operators. These modes are

$$V_{sp} \rightarrow \prod_m (m \alpha_1 \tilde{\alpha}_1)^{n_m} , \quad (B5)$$

evaluated at the world sheet coordinate $z = 1$. To lowest order in q , contribution of these modes to the one-loop amplitude (B3) is given by

$$q_2^{2n} n! \prod_m m^{n_m} , \quad (B6)$$

where $n \equiv \sum_m n_m$. After including (B4) (B6) and using the result discussed in Sec. IV B $\langle e^{ikX^0} \rangle_{X^0} \sim \frac{1}{E} e^{(\tau - \tau_\lambda)^2/\pi s}$ for heavy strings with $E = \sqrt{4N}$ ($N \equiv \sum_m m n_m$) and then squaring the amplitude,¹¹ we get

$$|A|^2 \propto \frac{1}{s} e^{2(\tau - \tau_\lambda)^2/\pi s} \frac{1}{N} \left(q_2^{2n} n! \prod_m m^{n_m} \right)^2 . \quad (B7)$$

Actually before we square the amplitude, we should integrate over the moduli $s_{1,2}$. Here to make a rough estimate we only integrated over a unit length of $s_{1,2}$ taking any value of $s_{1,2}$ as long as they are large. Since the amplitude does not change sign as we change $s_{1,2}$ when $s_{1,2}$ are large, the integration over other region will only make the amplitude bigger. But the effect of the small $s_{1,2}$ region is unclear and is not taken into account in this paper.

In (B7) the factors in the bracket grow rapidly as the level of the string states N increases. For the same level we also have the degeneracy of states characterized by the Hagedorn density. So after summing over all possible $\{n_m\}$ for (B7), the total energy emitted will diverge very rapidly as N increases.

¹¹The quantity we consider here is of order g^2 . There are also cross terms of order g between the one-loop and disk amplitude. For massive strings these terms become smaller due to the exponential fall-off of the disk amplitude as a function of E . Therefore for our purpose (to see the divergent behavior of the heavy strings emission) we do not consider them here.

REFERENCES

- [1] A. Sen, “Non-BPS states and branes in string theory,” arXiv:hep-th/9904207.
- [2] A. Sen, “Rolling tachyon,” JHEP **0204**, 048 (2002) [arXiv:hep-th/0203211].
- [3] A. Sen, “Tachyon matter,” JHEP **0207**, 065 (2002) [arXiv:hep-th/0203265].
- [4] A. Sen, “Field theory of tachyon matter,” Mod. Phys. Lett. A **17**, 1797 (2002) [arXiv:hep-th/0204143].
- [5] T. Okuda and S. Sugimoto, “Coupling of rolling tachyon to closed strings,” Nucl. Phys. B **647**, 101 (2002) [arXiv:hep-th/0208196].
- [6] B. Chen, M. Li and F. L. Lin, “Gravitational radiation of rolling tachyon,” JHEP **0211**, 050 (2002) [arXiv:hep-th/0209222].
- [7] N. Lambert, H. Liu and J. Maldacena, “Closed strings from decaying D-branes,” arXiv:hep-th/0303139.
- [8] D. Gaiotto, N. Itzhaki and L. Rastelli, “Closed strings as imaginary D-branes,” arXiv:hep-th/0304192.
- [9] A. Sen, “Open and closed strings from unstable D-branes,” arXiv:hep-th/0305011.
- [10] A. Sen, “Open-closed duality: Lessons from matrix model,” arXiv:hep-th/0308068.
- [11] A. Sen, “Time evolution in open string theory,” JHEP **0210**, 003 (2002) [arXiv:hep-th/0207105].
- [12] F. Larsen, A. Naqvi and S. Terashima, “Rolling tachyons and decaying branes,” JHEP **0302**, 039 (2003) [arXiv:hep-th/0212248].
- [13] E. Braaten, T. Curtright, G. Ghandour and C. B. Thorn, “Nonperturbative Weak Coupling Analysis Of The Liouville Quantum Field Theory,” Phys. Rev. Lett. **51**, 19 (1983).
- [14] E. Braaten, T. Curtright, G. Ghandour and C. B. Thorn, “Nonperturbative Weak Coupling Analysis Of The Quantum Liouville Field Theory,” Annals Phys. **153**, 147 (1984).
- [15] J. Polchinski, “Remarks On The Liouville Field Theory,” UTTG-19-90 *Presented at Strings '90 Conf., College Station, TX, Mar 12-17, 1990*
- [16] A. Strominger, “Open string creation by S-branes,” arXiv:hep-th/0209090.
- [17] M. Gutperle and A. Strominger, “Timelike boundary Liouville theory,” Phys. Rev. D **67**, 126002 (2003) [arXiv:hep-th/0301038].
- [18] A. Maloney, A. Strominger and X. Yin, “S-brane thermodynamics,” arXiv:hep-th/0302146.
- [19] S. Fredenhagen and V. Schomerus, “On minisuperspace models of S-branes,” arXiv:hep-th/0308205.

[20] P. Yi, “Membranes from five-branes and fundamental strings from Dp branes,” *Nucl. Phys. B* **550**, 214 (1999) [arXiv:hep-th/9901159].

[21] O. Bergman, K. Hori and P. Yi, “Confinement on the brane,” *Nucl. Phys. B* **580**, 289 (2000) [arXiv:hep-th/0002223].

[22] M. Gutperle and P. Kraus, “D-brane dynamics in the $c = 1$ matrix model,” arXiv:hep-th/0308047.

[23] K. Okuyama, “Comments on half S-branes,” arXiv:hep-th/0308172.

[24] C. G. Callan, I. R. Klebanov, A. W. Ludwig and J. M. Maldacena, “Exact solution of a boundary conformal field theory,” *Nucl. Phys. B* **422**, 417 (1994) [arXiv:hep-th/9402113].

[25] J. Polchinski and L. Thorlacius, “Free Fermion Representation Of A Boundary Conformal Field Theory,” *Phys. Rev. D* **50**, 622 (1994) [arXiv:hep-th/9404008].

[26] N. Ishibashi, “The Boundary And Crosscap States In Conformal Field Theories,” *Mod. Phys. Lett. A* **4**, 251 (1989).

[27] E. Witten, “Ground ring of two-dimensional string theory,” *Nucl. Phys. B* **373**, 187 (1992) [arXiv:hep-th/9108004].

[28] I. R. Klebanov and A. M. Polyakov, “Interaction of discrete states in two-dimensional string theory,” *Mod. Phys. Lett. A* **6**, 3273 (1991) [arXiv:hep-th/9109032].

[29] For more references, see e.g. N. Ohta, “Discrete states in two-dimensional quantum gravity,” arXiv:hep-th/9206012.

[30] S. Hwang, “Cosets as gauge slices in $SU(1,1)$ strings,” *Phys. Lett. B* **276**, 451 (1992) [arXiv:hep-th/9110039].

[31] J. M. Evans, M. R. Gaberdiel and M. J. Perry, “The no-ghost theorem for $AdS(3)$ and the stringy exclusion principle,” *Nucl. Phys. B* **535**, 152 (1998) [arXiv:hep-th/9806024].

[32] C. Itzykson and J. B. Zuber, “Quantum Field Theory,” McGraw Hill College Div (1980).

[33] P. Di Vecchia and A. Liccardo, “D branes in string theory. I,” arXiv:hep-th/9912161.

[34] F. Quevedo, “Lectures on string / brane cosmology,” *Class. Quant. Grav.* **19**, 5721 (2002) [arXiv:hep-th/0210292].

[35] P. Mukhopadhyay and A. Sen, “Decay of unstable D-branes with electric field,” *JHEP* **0211**, 047 (2002) [arXiv:hep-th/0208142].

[36] S. J. Rey and S. Sugimoto, “Rolling tachyon with electric and magnetic fields: T-duality approach,” *Phys. Rev. D* **67**, 086008 (2003) [arXiv:hep-th/0301049].

[37] S. J. Rey and S. Sugimoto, “Rolling of modulated tachyon with gauge flux and emergent fundamental string,” *Phys. Rev. D* **68**, 026003 (2003) [arXiv:hep-th/0303133].

[38] A. Sen, “Open-closed duality at tree level,” arXiv:hep-th/0306137.

[39] K. Nagami, “Closed string emission from unstable D-brane with background electric

field,” arXiv:hep-th/0309017.

[40] J. L. Karczmarek, H. Liu, J. Maldacena and A. Strominger, “UV finite brane decay,” arXiv:hep-th/0306132.

[41] J. Polchinski, “String Theory. Vol. 1: An Introduction To The Bosonic String,” Cambridge University Press (1999).

[42] M. B. Green, J. H. Schwarz and E. Witten, “Superstring Theory. Vol. 2: Loop Amplitudes, Anomalies And Phenomenology,” Cambridge University Press (1988).